A mathematical method for modeling the shape of apples
Part 1. Description of the method

L. Mieszkalski, J. Wojdalski

Department of Production Management and Engineering,
Warsaw University of Life Sciences, Nowoursynowska 166, 02-787 Warsaw, Poland
leszek_mieszkalski@sggw.pl; janusz_wojdalski@sggw.pl

Received: February 25, 2017; Accepted: May 10, 2017

Summary. This study proposes a mathematical method for modeling the shape of apples, locules and pericarps with the use of Bézier curves. The concave and convex parts of apples cv. *Ligol* were described with three smoothly-joined Bézier curves. Contours were described based on images of an apple rotated at intervals of 36° relative to its natural axis of symmetry. A 3D model was formed by Bézier curves positioned along the apple's meridians. The shape of the locule and the pericarp was described with the use of two smoothly-joined Bézier curves each, rotated relative to the apple's longitudinal axis.

Key words: apple, cv. *Ligol*, shape, locule, pericarp, Bézier curves, method, mathematical model.

INTRODUCTION

Agricultural and food raw materials are processed with the use of modern sorting and packaging methods to supply high-quality and defect-free products and to place innovative food products on the market [1-17]. Fruit deformations caused by dehydration were modeled by Aregawi et al. [18]. The implementation of innovative technical solutions has to be preceded by research on agricultural products. The relevant studies and experiments can be very costly, but they can be replaced by numerical models. Numerical models describe the geometric properties of agricultural products which are used to design and optimize production processes. The existing models of fruits, vegetables and seeds, which are based on regular shapes (sphere, ellipsoid), have been extensively described in the literature. In reality, the shape of fruits belonging to various cultivars does not always correspond to regular geometric figures due to low modeling accuracy. Biological objects are characterized by considerable irregularities and variations in shape, and they may be difficult to model [19-20]. Scientists search for new numerical methods that rely on advanced bioinformatics tools to accurately model the shape of biological materials. The geometric properties of biological objects are simulated with computer-aided design (CAD) tools [21-23]. Accurate models of biological objects that account for malformations and anatomic anomalies are still difficult to generate. There is a general scarcity of studies analyzing the shape and dimensions of biological objects. Various methods have been used to develop 3D models of agricultural and food raw materials, including machine vision, 3D scanning and mathematical modeling [19, 24-32]. Computer image analyses of fruit, including apples, constitute a separate group of studies [11, 33-43]. Computer graphics and differential geometry methods offer interesting alternatives for modeling the shape of biological objects [44-46]. Mieszkalski [47] proposed a mathematical model for describing the shape of apples cv. *Ligol* and *Jonagored* based on Bézier curves. In the presented model, the values of the parameters determining the basic geometric properties and the shape of fruits (within a species) can be modified, which supports modeling of geometric solids with sufficient accuracy for practical applications. The cited study relied on the findings of Rosell and Sanz [37] and Hongbo et al. [48].

The aim of this study was to develop a mathematical method for modeling the shape of apples cv. *Ligol* and their anatomical parts, the pericarp and the locule, with the use of Bézier curves.

MATERIALS

The study was performed on apples cv. *Ligol* characterized by spherical and conical shape. Apples were purchased in a wholesale market in Bronisze (Poland) and stored indoors at a constant temperature of 19°C and relative air humidity of 60%. Unbruised apples that differed in shape (Fig. 1) from the previously studied apples [47] were selected from a batch of 50 fruits.

Fig. 1. An apple cv. *Ligol* selected for modeling, photographed in 10 positions.

The basic dimensions of the analyzed apple (length, width, thickness; depth of the pedicel cavity h_1 and depth of the calyx basin h_2 – Figure 2) were measured with a caliper to the nearest 0.1 mm (Table 1).

The apple was photographed in a test stand presented in Figure 3. The apple was held by two clamps in its natural axis of symmetry. The line connecting the pedicel cavity with the calyx basin formed the apple's natural axis of symmetry. The bottom clamp held the calyx basin, and the top clamp pressed down on the pedicel cavity. The apple was rotated at intervals of 36° to produce 10 photographs. Photographs were taken with the Panasonic LUMIX DMC-TZ3 camera. The lens was placed at a distance of 400 mm from the photographed object. Images with a resolution of 2560 x 1920 pixels were stored in JPEG files.

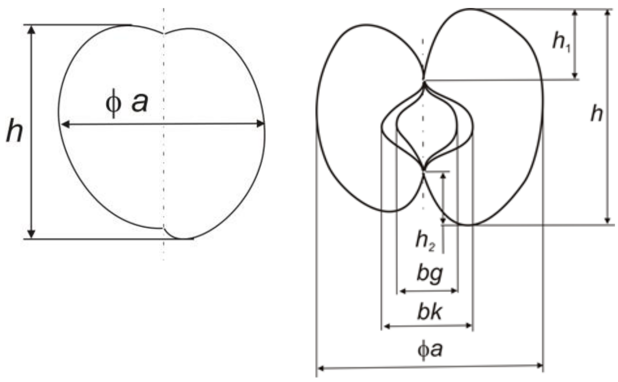

Fig. 2. Basic dimensions of an apple.

Table 1. Basic dimensions of the modeled apple

Parameter	Symbol	Value [mm]
Length	h	80.3
Width	b_1	88.5
Thickness	b_2	86.2
Depth of pedicel cavity	h_1	10.6
Depth of calyx basin	h_2	15.4

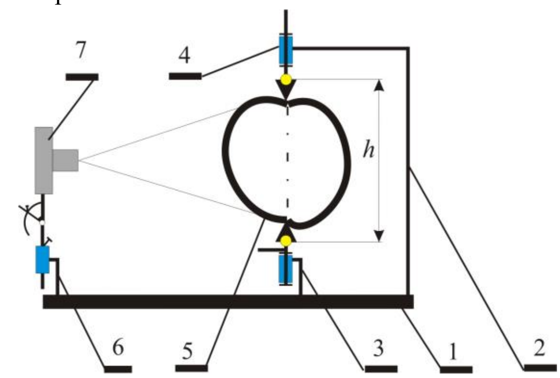

Fig. 3. Test stand: 1 – base, 2 – arm, 3 – bottom clamp, 4 – top clamp, 5 – apple, 6 – camera mount, 7 - camera

Every image was cropped and scaled. Images were loaded into the *Inkscape* graphic program, placed in a coordinate system, and three smoothly-joined Bézier curves were fitted to the image (Fig. 4). The intersection of the apple's natural axis of symmetry and the *x* axis, which was adjacent to the lower part of the apple, marked the beginning of the coordinate system. An apple is a solid with concave and convex surface. The position of nodes *Ax, Ay, Az, Cx, Cy, Cz* of Bézier curves was determined based on the values of h_1 and h_2.

The apple was halved to determine the shape of the locule and the pericarp. These anatomical features were modeled with two smooth-joined Bézier curves each (Fig. 5).

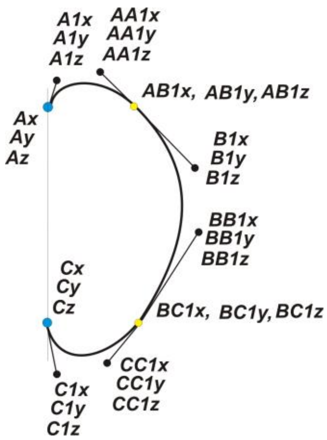

Fig. 4. Determination of the nodes and control points of three smooth-joined Bézier curves describing the contour of an apple

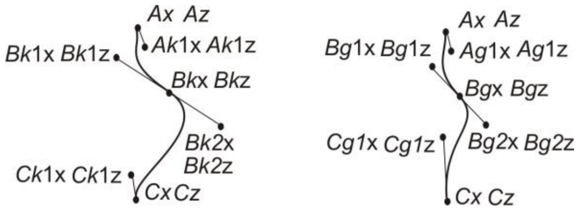

Fig. 5. Determination of the nodes and control points of two smooth-joined Bézier curves describing the external surface of the locule, and two smooth-joined Bézier curves describing the external surface of the pericarp.

MODEL DESCRIBING THE CONTOURS OF AN APPLE, LOCULE AND PERICARP WITH THE USE OF BÉZIER CURVES

The contours of an apple, its locule and pericarp were described by Bézier curves (third degree polynomials) with the use of matrix equations of the coordinates of contour points (Fig. 4, Fig. 5).

$$xn_t = T \cdot M \cdot Px^T \cdot \cos\left(\frac{\alpha n \cdot \pi}{180}\right), \quad (1)$$

$$yn_t = T \cdot M \cdot Py^T \cdot \sin\left(\frac{\alpha n \cdot \pi}{180}\right), \quad (2)$$

$$zn_t = T \cdot M \cdot Pz^T , \quad (3)$$

where:
the vector of parameter t has the following form:

$$T = \left[\left(\frac{t}{N}\right)^3 \quad \left(\frac{t}{N}\right)^2 \quad \frac{t}{N} \quad 1\right], \quad (4)$$

the Bézier basis matrix has the following form:

$$M = \begin{bmatrix} -1 & 3 & -3 & 1 \\ 3 & -6 & 3 & 0 \\ -3 & 3 & 0 & 0 \\ 1 & 0 & 0 & 0 \end{bmatrix}. \quad (5)$$

Geometry matrices Pax, Pay and Paz of the top part (A) of the apple are presented below:

$$Pax = [Ax \;\; Anx \;\; AAnx \;\; ABnx], \quad (6)$$

$$Pay = [Ay \;\; Any \;\; AAny \;\; ABny], \quad (7)$$

$$Paz = [Az \;\; Anz \;\; AAnz \;\; ABnz], \quad (8)$$

Geometry matrices Pbx, Pby and Pbz of the middle part (B) of the apple are presented below:

$$Pbx = [ABnx \;\; Bnx \;\; BBnx \;\; BCnx], \quad (9)$$

$$Pby = [ABny \;\; Bny \;\; BBny \;\; BCny], \quad (10)$$

$$Pbz = [ABnz \;\; Bnz \;\; BBnz \;\; BCnz], \quad (11)$$

Geometry matrices Pcx, Pcy and Pcz of the bottom part (C) of the apple are presented below:

$$Pcx = [BCnx \;\; CCnx \;\; Cnx \;\; Cx], \quad (12)$$

$$Pcy = [BCny \;\; CCny \;\; Cny \;\; Cy], \quad (13)$$

$$Pcz = [BCnz \;\; CCnz \;\; Cnz \;\; Cz]. \quad (14)$$

The following matrices were derived from equations (1, 2, 3 and 6 to 14):

matrices of Bézier curves $xA1$, …, $xA10$; $yA1$, …, $yA10$, $zA1$, …, $zA10$ describing the top part (A) of the apple,

matrices of Bézier curves $xB1$, …, $xB10$; $yB1$, …, $yB10$, $zB1$, …, $zB10$ describing the middle part (B) of the apple,

matrices of Bézier curves $xC1$, …, $xC10$; $yC1$, …, $yC10$, $zC1$, …, $zC10$ describing the bottom part (C) of the apple.

The *augment* function was used to connect the rows of matrices of Bézier curves describing apple parts *A, B, C,* producing matrices *XA, YA, ZA, XB, YB, ZB, XC, YC, ZC*:

XA = augment(xA1, xA2, …, xA10), (15)

YA = augment(yA1, yA2, …, yA10), (16)

ZA = augment(zA1, zA2, …, zA10), (17)

XB = augment(xB1, xB2, …, xB10), (18)

YB = augment(yB1, yB2, …, yB10), (19)

ZB = augment(zB1, zB2, …, zB10), (20)

XC = augment(xC1, xC2, …, xC10), (21)

YC = *augment*(*yC*1, *yC*2, ..., *yC*10), (22)

$$ZC = \text{augment}(zC1, zC2, ..., zC10). \quad (23)$$

The columns of matrices *XA, YA, ZA, XB, YB, ZB, XC, YC, ZC* were connected using the *stack* function to produce matrices *X*1, *Y*1, *Z*1:

$$X1 = stack(XA, XB, XC), \quad (24)$$

$$Y1 = stack(YA, YB, YC), \quad (25)$$

$$Z1 = stack(ZA, ZB, ZC), \quad (26)$$

Matrices *X*1, *Y*1, *Z*1 were used to develop a 3D model describing the external surface of the apple.

For *N* – number of parallels relative to one Bézier curve, *n* – number of a Bézier curve. The contour of the apple was described by three joined Bézier curves. Bézier curves for ten positions of the apple were joined at nodes inside the pedicel cavity and the calyx basin. The joined Bézier curves were smoothed at nodes on the apple contour by positioning the control points of the joined curves on the same straight line.

Geometry matrices *Pkax* and *Pkaz* of the first Bézier curve describing the locule are presented below:

$$Pkax = [Ax\ \ Ak1x\ \ Bk1x\ \ Bkx], \quad (27)$$

$$Pkaz = [Az\ \ Ak1z\ \ Bk1z\ \ Bkz]. \quad (28)$$

The vector of parameter *t*1 has the following form:

$$T = \left[\left(\frac{t1}{N}\right)^3 \left(\frac{t1}{N}\right)^2 \ \frac{t1}{N}\ \ 1\right]. \quad (29)$$

Geometry matrices *Pkbx* and *Pkbz* for the second Bézier curve describing the locule are presented below:

$$Pkbx = [Bkx\ \ Bk2x\ \ Ck1x\ \ Cx], \quad (30)$$

$$Pkbz = [Bkz\ \ Bk2z\ \ Ck1z\ \ Cz]. \quad (31)$$

The following matrices were derived from equations (1, 2 and 27 to 31):

matrices of the first Bézier curve describing the locule *xAk*1, *zAk*1,

matrices of the second Bézier curve describing the locule *xAk*2, *zAk*2.

Geometry matrices *Pgax* and *Pgaz* of the first Bézier curve describing the pericarp are presented below:

$$Pgax = [Ax\ \ Ag1x\ \ Bg1x\ \ Bgx], \quad (32)$$

$$Pgaz = [Az\ \ Ag1z\ \ Bg1z\ \ Bgz]. \quad (33)$$

The vector of parameter *t*1 has the following form:

$$T = \left[\left(\frac{t1}{N}\right)^3 \left(\frac{t1}{N}\right)^2 \ \frac{t1}{N}\ \ 1\right]. \quad (34)$$

Geometry matrices *Pgbx* and *Pgbz* of the second Bézier curve describing the pericarp are presented below:

$$Pgbx = [Bgx\ \ Bg2x\ \ Cg1x\ \ Cx], \quad (35)$$

$$Pgbz = [Bgz\ \ Bg2z\ \ Cg1z\ \ Cz]. \quad (36)$$

The following matrices were derived from equations (1, 2 and 32 to 36):

matrices of the first Bézier curve describing the pericarp *xAg*1, *zAg*1,

matrices of the second Bézier curve describing the pericarp *xAg*2, *zAg*2.

The first Bézier curve and, consequently, the second Bézier curve were rotated to produce solids representing the locule and the pericarp. The matrix equations for solids produced by the rotation of the first Bézier curve have the following form:

$$XAk1_{t1,\ j} = xAk1_{t1} \cdot \sin(\phi_j), \quad (37)$$

$$YAk1_{t1,\ j} = xAk1_{t1} \cdot \cos(\phi_j), \quad (38)$$

$$ZAk1_{t1,\ j} = zAk1_{t1}, \quad (39)$$

where:

$$\phi_j = \frac{2 \cdot \pi \cdot j}{N}. \quad (40)$$

The range of variables was written in vector 41:

$$\begin{bmatrix} t \\ j \\ t1 \end{bmatrix} = \begin{bmatrix} 0 \ldots N \\ 0 \ldots N \\ 0 \ldots N-1 \end{bmatrix}. \quad (41)$$

A similar approach was used to derive the matrix equations of solids produced by the rotation of the second

Bézier curve $XAk2_{t,j}$, $YAk2_{t,j}$, $ZAk2_{t,j}$. The matrix equations of coordinates $XAg1_{t1,j}$, $YAg1_{t1,j}$, $ZAg1_{t1,j}$ and $XAg2_{t,j}$, $YAkg2_{t,j}$, $ZAg2_{t,j}$ of points on the first and second Bézier curves were derived to describe the pericarp. The *stack* function was used to connect the columns of matrices of Bézier curves describing the locule:

$$Xka = stack(XAk1, XAk2), \quad (42)$$

$$Yka = stack(YAk1, YAk2), \quad (43)$$

$$Zka = stack(ZAk1, ZAk2), \quad (44)$$

and the pericarp:

$$Xga = stack(XAg1, XAg2), \quad (45)$$

$$Yga = stack(YAg1, YAg2), \quad (46)$$

$$Zga = stack(ZAg1, ZAg2). \quad (47)$$

Matrices *Xka, Yka* and *Zka* were used to develop a 3D model of the external surface of the locule, and matrices *Xga, Yga* and *Zga* were used to develop a 3D model of the external surface of the pericarp.

CONCLUSIONS

In the proposed method, Bézier curves are used to generate mathematical models of the shape of apples. The concave and convex parts of an apple are described with three smooth-joined Bézier curves. Contours are described with the use of photographs of an apple rotated at intervals of 36° relative to its natural axis of symmetry. A 3D model of an apple is formed by Bézier curves positioned along the apple's meridians. The shape of the locule and the pericarp is described with the use of two smooth-joined Bézier curves that are rotated relative to the apple's longitudinal axis.

REFERENCES

1. **Abbott J. A., 1999.** Quality measurement of fruits and vegetables. Postharvest Biology and Technology, 15(3), 207-225.
2. **Anderson E. R. Cuccia, D. J. & Durkin A. J. 2007, February.** Detection of bruises on Golden Delicious apples using spatial-frequency-domain imaging. In Biomedical Optics (BiOS) 2007 (pp. 64301O-64301O). International Society for Optics and Photonics.
3. **Blasco J. Aleixos N. Gómez-Sanchis J. & Moltó E., 2009.** Recognition and classification of external skin damage in citrus fruits using multispectral data and morphological features. Biosystems Engineering, 103(2), 137-145.
4. **Chen Y. R. Chao, K. & Kim M. S. 2002.** Machine vision technology for agricultural applications. Computers and Electronics in Agriculture, 36(2), 173-191.
5. **Czernyszewicz E., 2008**. The importance of some selected qualitative features of apples for buyers (Ważność wybranych cech jakościowych jabłek dla konsumentów). ŻYWNOŚĆ. Nauka. Technologia. Jakość, 1 (56), 114 – 125
6. **Du C. J. & Sun D. W., 2004**. Recent developments in the applications of image processing techniques for food quality evaluation. Trends in Food Science & Technology, 15(5), 230-249.
7. **Golpira H. & Golpîra H., 2013.** Application of signal processing technique for the modification of a fruit sorting machine. International Journal of Advanced Mechatronic Systems, 5(2), 122-128.
8. **Gołacki K. & Kołodziej P., 2011.** Impact testing of biological material on the example of apple tissue. TEKA Kom. Mot. i Energ. Roln. – OL PAN, 11c, 74-82
9. **Kavdır I. & Guyer D. E., 2004.** Comparison of artificial neural networks and statistical classifiers in apple sorting using textural features. Biosystems Engineering, 89(3), 331-344.
10. **Leemans V. & Destain M. F., 2004.** A real-time grading method of apples based on features extracted from defects. Journal of Food Engineering, 61(1), 83-89.
11. **López-García F. Andreu-García G. Blasco J. Aleixos N. & Valiente J. M., 2010.** Automatic detection of skin defects in citrus fruits using a multivariate image analysis approach. Computers and Electronics in Agriculture, 71(2), 189-197.
12. **Mebatsion H. K. Verboven P. Ho Q. T. Verlinden B. E. & Nicolaï B. M., 2008.** Modelling fruit (micro) structures, why and how?. Trends in food science & technology, 19(2), 59-66.
13. **Pakrashi V. O'Connor A. J. & Schoefs F., 2007, July.** An image analysis based damage classification methodology. In Applications of Statistics and Probability in Civil Engineering: Proceedings of the 10th International Conference, ICASP10, Tokyo, Japan, 31 July-3 August 2007. Taylor & Francis.
14. **Pieczywek P. M. & Zdunek A., 2012.** Automatic classification of cells and intercellular spaces of apple tissue. Computers and Electronics in Agriculture, 81, 72-78.

15. **Shahin M. A. Tollner E. W. McClendon R. W. & Arabnia H. R., 2002.** Apple classification based on surface bruises using image processing and neural networks. Transactions of the ASAE, 45(5), 1619.
16. **Unay D. & Gosselin, B., 2005, September.** Artificial neural network-based segmentation and apple grading by machine vision. In IEEE International Conference on Image Processing 2005 (Vol. 2, pp. II-630). IEEE.
17. **Unay D. & Gosselin B., 2006.** Automatic defect segmentation of 'Jonagold'apples on multi-spectral images: A comparative study. Postharvest Biology and Technology, 42(3), 271-279.
18. **Aregawi W. A. Abera M. K. Fanta S. W. Verboven, P. &Nicolai B., 2014.** Prediction of water loss and viscoelastic deformation of apple tissue using a multiscale model. Journal of Physics: Condensed Matter, 26(46), 464111.
19. **Goñi S.M. & Purlis E., 2010.** Geometric modelling of heterogeneous and complex foods. Journal of Food Engineering, 4, 97, 547-554.
20. **Ho Q. T. Carmeliet J. Datta A. K. Defraeye T. Delele M. A. Herremans E. & Van Liedekerke P., 2013.** Multiscale modeling in food engineering. Journal of Food Engineering, 114(3), 279-291.
21. **Balcerzak K. Weres J. Górna K. & Idziaszek P., 2015.** Modeling of agri-food products on the basis of solid geometry with examples in Autodesk 3DS Max and finite element mesh generation. Journal of Research and Applications in Agricultural Engineering, 60(2), 5-8.
22. **Weres J. Olek W. Kujawa S. & Siatkowski M., 2014a.** Integration of software components for determination and analysis of properties of agri-food and forest products. Journal of Research and Applications in Agricultural Engineering, 59(1), 159-163.
23. **Weres J. Kiecana M. & Balcerzak K., 2014b.** Two approaches to representing agri-food product geometry – an original software for constructing finite element models and the 3ds max approach. Journal of Research and Applications in Agricultural Engineering, 59(1), 155-158.
24. **Anders A. Markowski P. & Kaliniewicz Z., 2014**. Badanie właściwości geometrycznych i fizycznych owoców wybranych odmian gruszy na podstawie modeli numerycznych uzyskanych za pomocą skanera 3D. Zeszyty Problemowe Postępów Nauk Rolniczych, 577, 3-12.
25. **Gielis J., 2003.** A generic geometric transformation that unifies a wide range of natural, and abstract shapes. American Journal of Botany, 90(3), 333-338.
26. **Gielis J. & Gerats T., 2004.** A botanical perspective on modeling plants and plant shapes in computer graphics. International Conference on Computer, Communication and Control Technologies. Austin, Texas.
27. **Goñi S.M. Purlis E. & Salvadori V.O., 2007.** Three-dimensional reconstruction of irregular foodstuffs. Journal of Food Engineering 82, 536-547.
28. **Jancsók P. Clijmans L. Nicolai B.M. & De Baerdemaeker J., 2001.** Investigation of the effect of shape on the acoustic response of 'Conference' pears by finite element modelling. Postharvest Biology and Technology 23, 1-12.
29. **Kafashan J., Tijskens B. Moshou D. Bravo C. De Baerdemaeke J. & Ramon H., 2006.** A new method to model a 3D shape of biomaterials for using in post-harvest modelling. Control Applications in Post-Harvest and Processing Technology (CAPPT 2006), 223.
30. **Kim G. W. Do G. S. Bae Y. & Sagara Y., 2008.** Analysis of mechanical properties of whole apple using finite element method based on three-dimensional real geometry. Food Science and Technology Research, 14(4), 329-336.
31. **Mieszkalski L., 2014.** Mathematical model of the shape of broad seed. Ann. Warsaw Univ. Life Sci. – SGGW, Agricult. 63, 41-48.
32. **Scheerlinck N. Marquenie D. Jancsok P.T. Verboven P. Moles C.G. Banga J.R. & Nicolai B.M., 2004.** A model-based approach to develop periodic thermal treatments for surface decontamination of strawberries. Postharvest Biology and Technology, 34, 39-52.
33. **Brosnan T. & Sun D. W., 2004.** Improving quality inspection of food products by computer vision - a review. Journal of Food Engineering, 61(1), 3-16.
34. **Costa C. Antonucci F., Pallottino F. Aguzzi J. Sun D. W. Menesatti P., 2011.** Shape analysis of agricultural products: a review of recent research advances and potential application to computer vision. Food and Bioprocess Technology, 4(5), 673-692.
35. **Cubero S. Aleixos N. Moltó E. Gómez-Sanchis J. & Blasco J., 2011**. Advances in machine vision applications for automatic inspection and quality evaluation of fruits and vegetables. Food and Bioprocess Technology, 4(4), 487-504.
36. **Davies E. R., 2009.** The application of machine vision to food and agriculture: a review. The Imaging Science Journal, 57(4), 197-217.
37. **Rosell J. R. & Sanz R., 2012.** A review of methods and applications of the geometric characterization of

tree crops in agricultural activities. Computers and Electronics in Agriculture, 81, 124-141.

38. **Kleynen O. Leemans V. & Destain M. F., 2005.** Development of a multi-spectral vision system for the detection of defects on apples. Journal of Food Engineering, 69(1), 41-49.
39. **Kodagali J. A. & Balaji S., 2012.** Computer vision and image analysis based techniques for automatic characterization of fruits-a review. International Journal of Computer Applications, 50(6), 6-12.
40. **Mahendran R. Jayashree G.C. & Alagusundaram K., 2012.** Application of Computer Vision Technique on Sorting and Grading of Fruits and Vegetables. J Food Process & Technology S1-001. doi:10.4172/2157-7110.S1-001
41. **Moreda G. P. Muñoz M. A. Ruiz-Altisent M. & Perdigones A., 2012.** Shape determination of horticultural produce using two-dimensional computer vision–A review. Journal of Food Engineering, 108(2), 245-261.
42. **Narendra V. G. & Hareesha K. S., 2010.** Quality inspection and grading of agricultural and food products by computer vision - A Review. International Journal of Computer Applications, 2(1), 43-65.
43. **Patel, K. K., Kar, A., Jha, S. N., & Khan, M. A., 2012.** Machine vision system: a tool for quality inspection of food and agricultural products. Journal of Food Science and Technology, 49(2), 123-141.
44. **Foley J. D. Van Dam A. Feiner S.K. Hughes J.F. & Phillips R. L., 2001.** Wprowadzenie do grafiki komputerowej. WNT, Warszawa. ISBN 83-204-2662-6.
45. **Kiciak P., 2000.** Podstawy modelowania krzywych i powierzchni. Zastosowania w grafice komputerowej. WNT, Warszawa. ISBN 83-204-2464-X.
46. **Opera J., 2002.** Geometria różniczkowa i jej zastosowanie. Wydawnictwo Naukowe PWN, Warszawa. ISBN 83-01-13875-0
47. **Mieszkalski L., 2015.** Komputerowe wspomaganie modelowania kształtu jabłek. Acta Sci. Pol. Technica Agraria, 14(3-4), 19-31.
48. **Hongbo S., Dai Shiming G. X., Shenglian L. & Yanan W., 2008.** Geometry Modeling and Visualization of the Apple Fruit. *Chinese Agricultural Science Bulletin*, *10*, 116.